

High-frequency damping of collective excitations in fermion systems. II. Damping of zero sound in normal liquid ^3He

A. Holas

Institute of Physical Chemistry of the Polish Academy of Sciences, Kasprzaka 44, 01-224 Warsaw, Poland

K. S. Singwi

Department of Physics and Astronomy, Northwestern University, Evanston, Illinois 60208

(Received 21 October 1988)

The polarization potential approach of Aldrich and Pines to treat the elementary excitations in liquid ^3He is here extended by an explicit many-body calculation of the two-particle-hole pair contribution to the imaginary part of the proper polarizability, as outlined in paper I and using a physically reasonable ansatz. The result is then used to calculate the line shape of the zero-sound mode in liquid ^3He . The calculated dispersion and width of the zero-sound mode for different values of pressure are compared with the recent neutron inelastic scattering experiments of Scherm *et al.* [Phys. Rev. Lett. **59**, 217 (1987)]. The agreement between theory and experiment is quite satisfactory for small wave numbers; for large wave numbers the cause of the discrepancy between theory and experiment is critically examined. A possible modification of the effective potential between ^3He quasiparticles is suggested.

I. INTRODUCTION

Many years ago Landau¹ had predicted that a Fermi liquid, like liquid ^3He , could sustain at absolute zero temperature, a collective mode which is phononlike, which he called zero sound in order to distinguish it from ordinary sound. The condition for the existence of the latter is $\omega\tau \ll 1$, whereas for the former the condition is $\omega\tau \gg 1$; ω being the frequency of the sound and τ the mean collision time of the particles. Landau's prediction was later verified by Sköld *et al.*² through neutron inelastic-scattering experiments. These authors measured the dispersion of zero sound in the region of wave number transcending the validity of the Landau theory. The dispersion was found to be anomalous and to flatten for wave numbers $k > 0.8 \text{ \AA}^{-1}$. This and other discoveries led to some considerably activity³ towards a microscopic understanding of liquid ^3He . The interest in this system has been further heightened by recent neutron inelastic-scattering experiments of Scherm *et al.*⁴ at 120 mK. These experiments have furnished us, for the first time, with very detailed information both on the dispersion and damping of zero sound as a function of the density (or pressure) of the liquid. Their significance lies in the fact that they serve as a touchstone for the microscopic theories of excitations in Fermi liquids.

Since ^3He is a very dense liquid, a semiphenomenological theory seems to be the only possible way of describing this system. Of the known semiphenomenological theories of excitations in liquid ^3He , perhaps the most successful one is the so-called polarization-potential approach of Aldrich and Pines.⁵ One of the most remarkable successes of this approach has been that it predicted both the anomalous dispersion of zero sound and its flattening in the large-wave-number region before it was ex-

perimentally seen. More recently, Hess and Pines⁶ (hereafter referred to as HP), using the approach of Ref. 5, have been able to explain quantitatively the experimental results of Scherm *et al.*⁴ on dispersion as a function of pressure. To achieve this, these authors obviously had to adjust the parameters of their effective potential with pressure. In spite of its great success, the polarization-potential approach of Pines and co-workers is incapable of explaining the damping of zero sound. In fact, no damping mechanism exists in their approach. On the other hand, experiments of Ref. 4 show that the damping of the zero-sound mode is substantial and increases both with wave number and pressure. The primary aim of the present paper is to understand the mechanism of damping of the zero-sound mode and calculate its line shape from microscopic considerations.

For wave numbers less than a certain critical wave number k_c at which the zero-sound mode touches the particle-hole continuum, there are only two possible channels of decay. One channel corresponds to the decay of one phonon into two phonons, and the other corresponds to the simultaneous excitation of two or more particle-hole pairs from the Fermi sea. The former mechanism can easily be ruled out because the anomalous dispersion, which is responsible for the linewidth in this case, disappears with increasing density, whereas the observed width increases with density. Besides, it predicts a linewidth which is almost two orders of magnitude smaller than what is observed. Therefore, the damping of zero sound must arise from processes involving multi-particle-hole excitations. The latter even in the lowest approximation (two-pair excitations) are fairly complex to calculate, and almost impossible to model.

A very similar situation exists in the damping of plasmons in an electron gas. This problem was treated

some time ago, as we have seen in paper I,⁷ by Glick and Long.⁸ In contrast to the electron-gas problem, the damping in ³He is quite large and one cannot use the simplified formulas for the linewidth Γ , derived by assuming that $\Gamma \ll \omega_0(k)$, $\omega_0(k)$ being the frequency of the mode. One is required to calculate the full dynamic form factor $S(k, \omega)$, and estimate both the position and the width from the line shape. Besides, one has the added problem of adapting to the ³He case, the calculation of two-particle-hole processes of Ref. 8, a calculation which was performed by evaluating the contribution of ten Feynman diagrams in the second order of the perturbation theory. Unfortunately, the latter cannot be straightforwardly applied to the Lennard-Jones-type of potential. The other difficulty is the large mass renormalization which exists in this problem. To circumvent these difficulties, we have adopted the attitude that the effective interaction between two ³He quasiparticles is some kind of pseudopotential, which, being weak, is amenable to a perturbation treatment. We, therefore, make the *ansatz* of replacing the bare interaction by an effective interaction when evaluating the Feynman graphs of Fig. 2 of Ref. 8. Also, we replace the bare mass m by an effective mass m^* in the propagators. Note that here m^* is independent of the momentum. The above *ansatz* is really not new and is, in fact, in the spirit of the polarization-potential theory of Pines and coworkers. For the effective potential between the quasiparticles we adopt the scalar polarization potential f_k^s of HP and use it to evaluate the two-particle-hole pair diagrams, which contribution, in the lowest order, is responsible for the damping of zero sound. Stated more explicitly, we extend the approach of HP by including, using microscopic considerations, the imaginary part of the two-pair contribution to the proper polarizability $\Pi(k, \omega)$. This contribution, which is solely responsible for the damping of zero sound, is impossible to model, as we shall see, because of its complicated dependence on frequency ω and on the form of the effective interaction $v(k)$.

It should be mentioned that a microscopic calculation of the dispersion and damping of zero sound in liquid ³He and its variation with pressure was first attempted by Glyde and Khanna.⁹ Their calculation was based on the theory of sound propagation in a dilute Fermi gas by Götffried and Pičman.¹⁰ It is doubtful that the latter theory can be applied to a dense system like liquid ³He. Besides, as we now know, the overall agreement with experiment is not very satisfactory.

II. DYNAMIC STRUCTURE FACTOR $S(k, \omega)$

The density-density response function, within the many-body perturbation theory, for a system of fermions interacting via a potential $v(k)$ can be written as

$$\chi(k, \omega) = \frac{\Pi(k, \omega)}{1 - v(k)\Pi(k, \omega)}, \quad (2.1)$$

where $\Pi(k, \omega)$ is the proper polarizability. The dynamic structure factor $S(k, \omega)$ is given by

$$S(k, \omega) = -\frac{1}{n\pi} \text{Im}\chi(k, \omega), \quad (2.2)$$

where n is the number density.

In the approach of HP, the function χ is written as

$$\chi(k, \omega) = \frac{\chi_{sc}(k, \omega)}{1 - \left[f_k^s + \frac{\omega^2}{k^2} h_k^s \right] \chi_{sc}(k, \omega)}, \quad (2.3)$$

where $\chi_{sc}(k, \omega)$ is the so-called screened response, and f_k^s is the Fourier transform of the effective symmetrized potential between ³He quasiparticles. The other term in the denominator takes care of the backflow. Our *ansatz* consists in making use of the parameters f_k^s and h_k^s in the following way:

$$v(k) = f_k^s \quad (2.4)$$

and

$$m^* = m + nh_0^s, \quad (2.5)$$

where m is the bare mass.

We now write the HP response χ of Eq. (2.3) in the form (2.1), i.e.,

$$\chi = \frac{\Pi_{HP}}{1 - v\Pi_{HP}} = \frac{\chi_{sc}}{1 - \left[f_k^s + \frac{\omega^2}{k^2} h_k^s \right] \chi_{sc}}. \quad (2.6)$$

Inverting (2.6) and using (2.4) we have

$$\Pi_{HP}(k, \omega) = \frac{\chi_{sc}(k, \omega)}{1 - \frac{\omega^2}{k^2} h_k^s \chi_{sc}(k, \omega)}. \quad (2.7)$$

Thus, within our *ansatz* and within the HP formulation, Eq. (2.7) gives the proper polarizability. For χ_{sc} and h_k^s , we use the expressions of HP. Equation (2.7) is reminiscent of a random-phase-approximation (RPA)-like expression for the proper polarizability, where the interaction is $(\omega^2/k^2)h_k^s$ and m in the Lindhard function χ_0 is replaced by m^* . It takes care of the contribution induced by the vector polarization potential.

In the frequency range of interest here and above the particle-hole continuum edge, the right-hand side of (2.7) according to Refs. 5 and 6 is purely real. We, therefore, consider Π_{HP} to play the role of the real part of the proper polarizability Π , while the imaginary part of Π is calculated in I within our *ansatz* of course. Since we shall confine ourselves to the frequency domain, where the asymptotic expression for $\text{Im}\Pi_{2p}$ can be used [see Eq. (2.1b) of paper I], we write

$$\Pi(k, \omega) = \Pi_{HP}(k, \omega) + i \text{Im}\Pi_{2p}(k, \omega), \quad (2.8)$$

where

$$\text{Im}\Pi_{2p}(k, \omega) = -\frac{m^*3n^2}{16\pi\hbar^6} k^4 P(Q) \frac{1}{Q^7}, \quad (2.9)$$

$$Q = Q(\omega) = \left[\frac{m^*\omega}{\hbar} \right]^{1/2}, \quad (2.10)$$

and

$$P(Q) = \frac{7}{15}v^2(Q) - \frac{2}{15}v(Q)Q \frac{dv(Q)}{dQ} + \frac{3}{15} \left[Q \frac{dv(Q)}{dQ} \right]^2. \quad (2.11)$$

The suffix $2p$ on Π is used to denote that we are considering only two-particle-hole pair contributions. Note that if $\text{Im}\pi_{2p} = 0$, we regain the HP expression (2.3) for χ . We have thus extended the HP approach by including the two-particle-hole pair contribution to multipair excitations. In the frequency range of interest here, the imaginary part of the HP expression for multipair excitations gives zero contribution. Also, note the simple dependence of $\text{Im}\Pi_{2p}$ on k and a very complicated dependence on ω via Q and $v(Q)$.

Using Eqs. (2.1), (2.2), and (2.7)–(2.11), it is straightforward to calculate $S(k, \omega)$ and thus the line shape of the zero-sound mode. From the line shape we determine the position of the maximum $\omega_0(k)$ and the full width $\Gamma(k)$ at half maximum. It is important to remember that now, because of the presence of damping, the position of $\omega_0(k)$, i.e., the dispersion of zero sound, would change from its value in the HP calculation. The more the damping, the greater is the change.

III. DISCUSSION OF RESULTS

A. HP Potential for $v(k)$

The r space potentials used by HP, have the form⁶

$$f(r^{\sigma\sigma'}) = \begin{cases} a^{\sigma\sigma'} [1 - (r/r_c^{\sigma\sigma'})^8] & \text{for } r < r_c^{\sigma\sigma'}, \\ b^{\sigma\sigma'} [(r_c^{\sigma\sigma'}/r)^{12} - (r_c^{\sigma\sigma'}/r)^6] & \text{for } r_c^{\sigma\sigma'} \leq r < r_t, \\ -(a_8/r^8 + a_6/r^6) & \text{for } r_t \leq r, \end{cases} \quad (3.1)$$

where $a_8 = 28\,400.5 \text{ \AA}^8 \text{ K}$, $a_6 = 10\,163.3 \text{ \AA}^6 \text{ K}$, and $r_t = 5.0 \text{ \AA}$ are parameters independent of pressure, while $r_c^{\sigma\sigma'}$, $a^{\sigma\sigma'}$, and $b^{\sigma\sigma'}$ are pressure dependent. Their values at $p = 0$ are, respectively, 3.00 \AA , 23.2 K , and 16.3 K for $\sigma\sigma' = \uparrow\downarrow$ and 3.03 \AA , 20.9 K , and 15.4 K for $\sigma\sigma' = \uparrow\uparrow$. For other pressures see Table II of Ref. 6. Interesting to us is f_k^s , the Fourier transform of the symmetrized potential,

$$v(k) = f_k^s = \int e^{ik \cdot r} \frac{1}{2} [f^{\uparrow\downarrow}(r) + f^{\uparrow\uparrow}(r)] d^3r. \quad (3.2)$$

We have recalculated f_k^s using Eqs. (3.1) and (3.2) and the dispersion of zero sound as given by the formulas of HP. We find that our results agree with theirs, which provides a check on our calculation. With $v(k)$ thus known, we have calculated $S(k, \omega)$ as mentioned in Sec. II. The results at saturated vapor pressure (SVP) are shown in Fig. 1(a) for some values of k . The scale along the y axis for $S(k, \omega)$ is in absolute units. Notice that the line shape of the zero-sound mode is quite broad and somewhat asymmetric and that the maximum falls off as k increases. Such plots were made for every pressure¹¹ and k . Peak position $\omega_0(k)$ and the width $\Gamma(k)$ as read from such curves are as shown in subsequent figures and are also

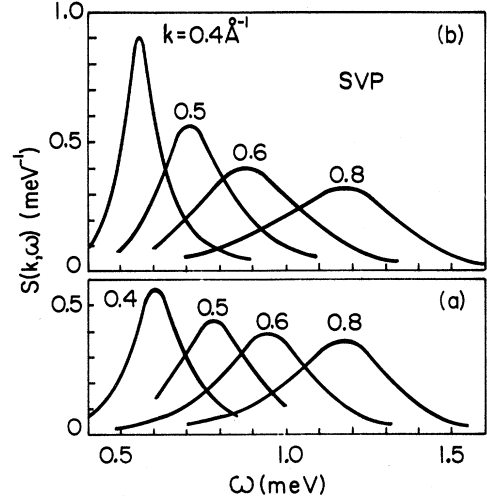


FIG. 1. Dynamic structure factor $S(k, \omega)$ vs ω at SVP for $k = 0.4, 0.5, 0.6,$ and 0.8 \AA^{-1} , calculated (a) with HP potential, and (b) with modified potential.

given in Table I.

Dispersion and width for four different values of pressure are shown, respectively, in Fig. 2(a) and Fig. 2(b) as continuous curves. Dashed-dotted curves denote the dispersion obtained without damping and are, therefore, the same as given by HP. Open squares are the experimental points of Ref. 4. Notice that the frequency $\omega_0(k)$ increases in the presence of damping, thus spoiling the good agreement with experiment obtained by HP without damping. The same situation prevails at all pressures.

For small wave numbers, the calculated widths are in good agreement with experiment, but with increasing wave number this agreement gets worse. However, in comparing theory with experiment, one should bear in mind that $\text{Im}\Pi_{2p}$, which determines the width, is a very sensitive function of the potential, effective mass, and frequency, as is seen from Eqs. (2.9)–(2.11). In view of this, the present agreement should be considered as remarkable, and an indication of the reasonableness of our ansatz. Part of the discrepancy between theory and experiment could very well be due to our use of the asymptotic formula. Also note that whenever the calculated width is large, there is a correspondingly large change in $\omega_0(k)$.

In order to understand the possible reasons for the calculated width being too small for larger values of k and for higher pressures, we decided to examine in greater detail some of the quantities entering in Eq. (2.7) for $\text{Im}\Pi_{2p}(k = 1 \text{ \AA}^{-1}; \omega)$. In Fig. 3(a) are shown the functions $v(Q(\omega))$, $P(Q(\omega))$, and $\text{Im}\Pi_{2p}(k = 1 \text{ \AA}^{-1}; \omega)$ as a function of ω at SVP; and in Fig. 3(b) are shown the same quantities for $p = 18 \text{ bar}$. From Fig. 2(b) and Table I, we see that at SVP the calculated value of Γ is $\approx 0.35 \text{ meV}$ at $k = 0.8 \text{ \AA}^{-1}$, and is about 30% less than the experimental value of 0.51 meV . The corresponding experimental value of $\omega_0(k)$ is 1.1 meV . We are, therefore, in-

TABLE I. Zero-sound energy $\omega_0(k)$ and width $\Gamma(k)$ in ${}^3\text{He}$. Results denoted by HP are the same as obtained by Hess and Pines (i.e., when damping is neglected). Our results: *A*—obtained with the HP potential; *B*, with modified potential. Experiment—from Ref. 4.

p (bar)	k (\AA^{-1})	$\omega_0(k)$ (meV)				$\Gamma(k)$ (meV)		
		HP	our <i>A</i>	our <i>B</i>	Expt.	Our <i>A</i>	Our <i>B</i>	Expt.
0	0.3	0.422	0.432	0.406	0.43	0.104	0.066	0.18
	0.4	0.582	0.606	0.554	0.57	0.188	0.132	0.17
	0.5	0.736	0.784	0.708	0.71	0.266	0.253	0.25
	0.6	0.874	0.947	0.878	0.83	0.313	0.384	0.25
	0.7	0.998	1.079	1.045	1.00	0.335	0.443	0.45
	0.8	1.070	1.179	1.178	1.09	0.347	0.441	0.51
	0.9	1.122	1.249	1.273	1.13	0.356	0.434	
	1.0	1.146	1.292	1.339	1.19	0.368	0.411	
5	1.1	1.156	1.316	1.381	1.19	0.378	0.403	
	0.3	0.531	0.565	0.509	0.55	0.197	0.090	0.22
	0.4	0.715	0.777	0.670	0.70	0.265	0.166	0.29
	0.5	0.884	0.964	0.825	0.83	0.283	0.269	0.38
	0.6	1.027	1.114	0.972	0.96	0.276	0.358	0.53
	0.7	1.138	1.226	1.100	1.14	0.264	0.400	0.57
	0.8	1.212	1.305	1.199	1.20	0.255	0.407	0.62
	10	0.4	0.805	0.878		0.79	0.256	
0.5		0.984	1.056		0.92	0.240		0.43
0.6		1.132	1.194		1.10	0.212		0.63
0.7		1.242	1.295		1.28	0.187		
0.8		1.315	1.364		1.28	0.171		
0.9		1.353	1.405		1.33	0.166		
1.0		1.363	1.425		1.38	0.172		
1.1		1.350	1.429		1.35	9.173		
18	0.4	0.909	0.974		0.89 ^a	0.218		0.32 ^a
	0.5	1.101	1.145		1.06 ^a	0.172		0.59 ^a
	0.6	1.257	1.281		1.33 ^a	0.121		0.67 ^a

^aExperiment is at $p = 20$ bar.

terested in the energy range from 0.85–1.35 meV in our calculation of $S(k, \omega)$. This corresponds to a value of Q in the range 1.30–1.64 \AA^{-1} . In the above energy range, we see from Fig. 3(a) that $v(Q(\omega))$ reaches the point where it crosses the energy axis and where its value is rather small. But the value of the function $P(Q(\omega))$ is quite large due to the value of the derivative of the potential being large. In this energy range, the function P changes by a factor of $\frac{1}{2}$. On the other hand, $\text{Im}\Pi_{2p}(k=1 \text{\AA}^{-1}, \omega)$ changes by a factor of $\frac{1}{12}$ over this range due to the occurrence of Q^7 in the denominator, which accounts for the factor $\frac{1}{6}$. From this we conclude that by changing the derivative of the potential in the above-mentioned range, we could make the width come closer to the experimental value. It is possible to do so without changing $v(k)$ at $k=0.8 \text{\AA}^{-1}$ and thus leaving the peak position practically unchanged.

The above situation gets much worse for higher pressures, as can be seen from an examination of Fig. 3(b) for $p=18$ bar. For example, at $k=0.6 \text{\AA}^{-1}$, the range of interest of energy is from 0.99–1.67 meV and of Q is from 1.70–2.33 \AA^{-1} . In this range, we see that $v(Q(\omega))$ starts from zero and is small negative and very flat, making

$P(Q(\omega))$ rather small. The value of P at $\omega=1.33$ meV is only 6% of its peak value. This is the reason why the calculated width is too small compared to experiment for higher pressures.

In view of the above analysis, we were tempted to make minor changes in the HP potential to see what effect they would have on the line shape. Besides, one would like to know whether these changes are consistent with the calculation of other properties of ${}^3\text{He}$ involving $v(k)$.

B. Modified potential

We modified the original HP potential [see Fig. 4(a) solid line] for two pressures SVP and 5 bar by adding a small correction shown as a dashed-dotted curve. The resulting potential is shown as a dashed curve in Fig. 4(a). The corresponding potentials in k space are shown in Fig. 4(b). A constraint was imposed on the modification such that the value of $v(k)$ at $k=0$ remains unchanged; i.e., the value of the Landau parameter F_s^0 remains the same.¹¹ At this stage, no physical significance should be

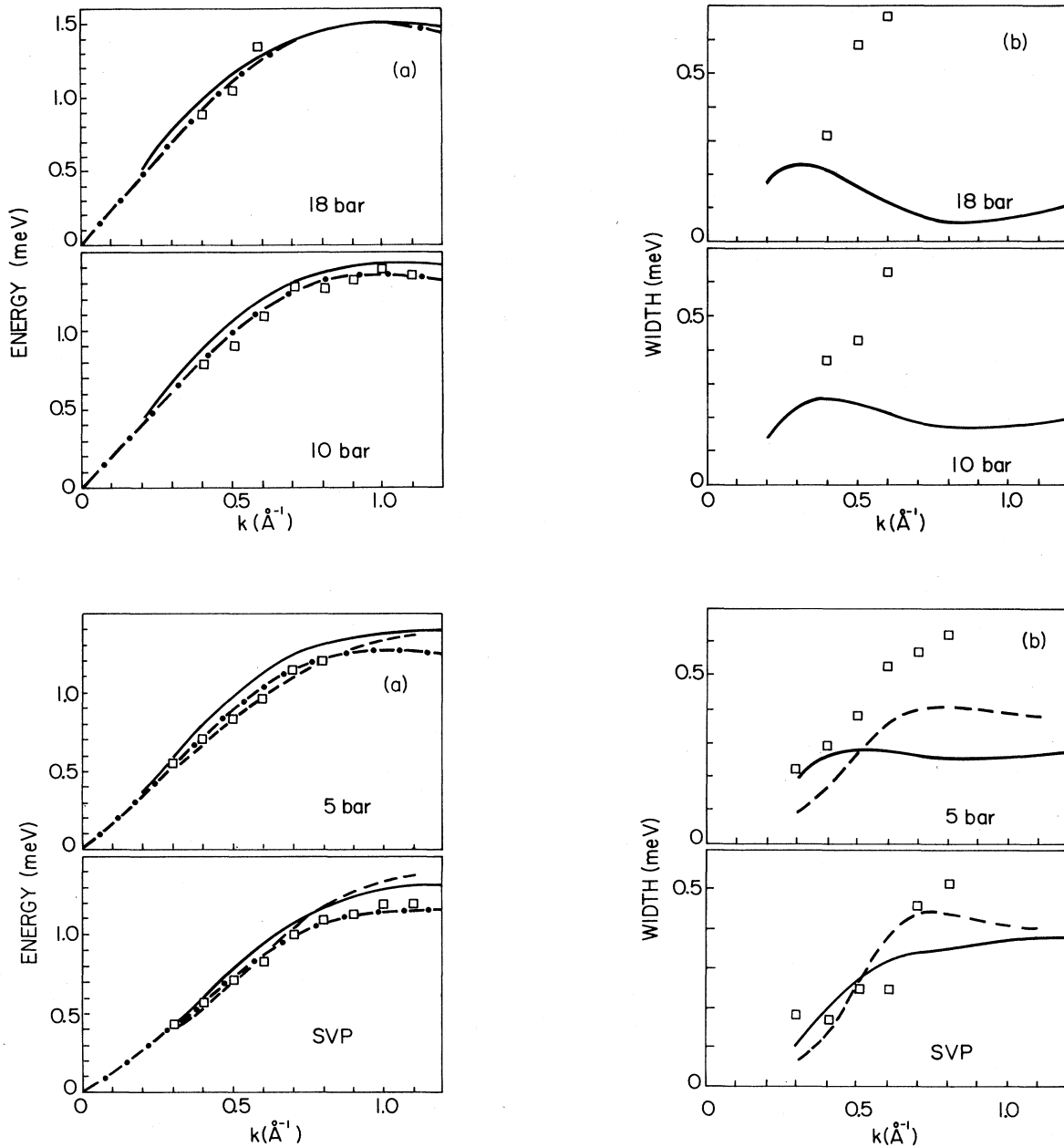


FIG. 2. Zero-sound energy $\omega_0(k)$ and full width $\Gamma(k)$ at half maximum vs k for various pressures. Solid lines, calculated with HP potential; dashed lines, with model potential; dashed-dotted lines, with HP potential when damping is neglected. Squares denote experimental points from Ref. 4. (Experimental points shown on 18-bar figure correspond to 20 bar.)

attached to these changes, which should be considered more in the nature of an exercise. Peak positions and widths were recalculated for the modified potentials, and are shown as dashed curves in Fig. 2, and are given in Table I as results *B*. We see that the peak position is shifted down due to the lowering of the main peak of $v(k)$, resulting in a better agreement with experiment. Also, the width agrees with experiment over a wider k range. The latter improvement is the result of the in-

creased slope of $v(k)$ in the vicinity of k values, where $v(k)=0$.

In Fig. 1(b) are shown the zero-sound line shapes at SVP for different values of k using the modified potential. A comparison with Fig. 1(a) shows that maximum of $S(k, \omega)$ decreases somewhat more rapidly with increasing k . Note that the calculated line shapes are in absolute scale, and are in remarkably good agreement with the corresponding experimental curves as seen from Fig. 1 of

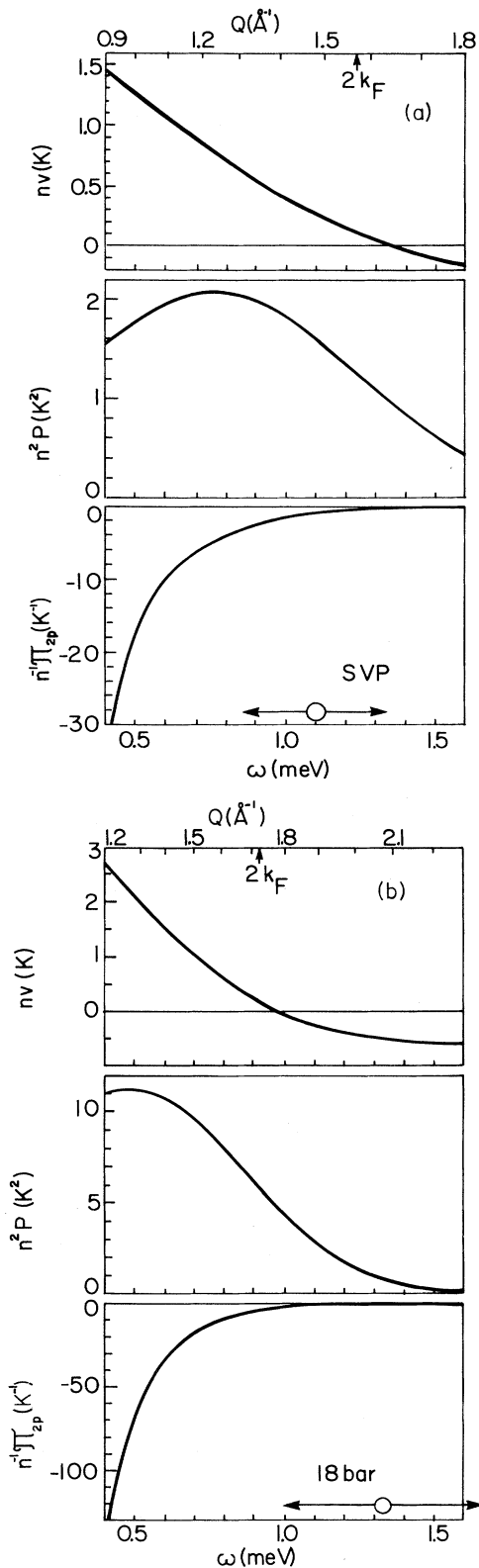


FIG. 3. Functions $nv(Q(\omega))$, $n^2P(Q(\omega))$, and $n^{-1}\text{Im}\Pi_{2p}(1\text{ \AA}^{-2}, \omega)$ vs ω (a) at SVP and (b) at 18 bar. The arrow indicates the full width of zero sound at $k=0.8\text{ \AA}^{-1}$ for SVP and $k=0.6\text{ \AA}^{-1}$ for 18 bar. Note: kelvins are used as energy unit for functions plotted here and in Fig. 4.

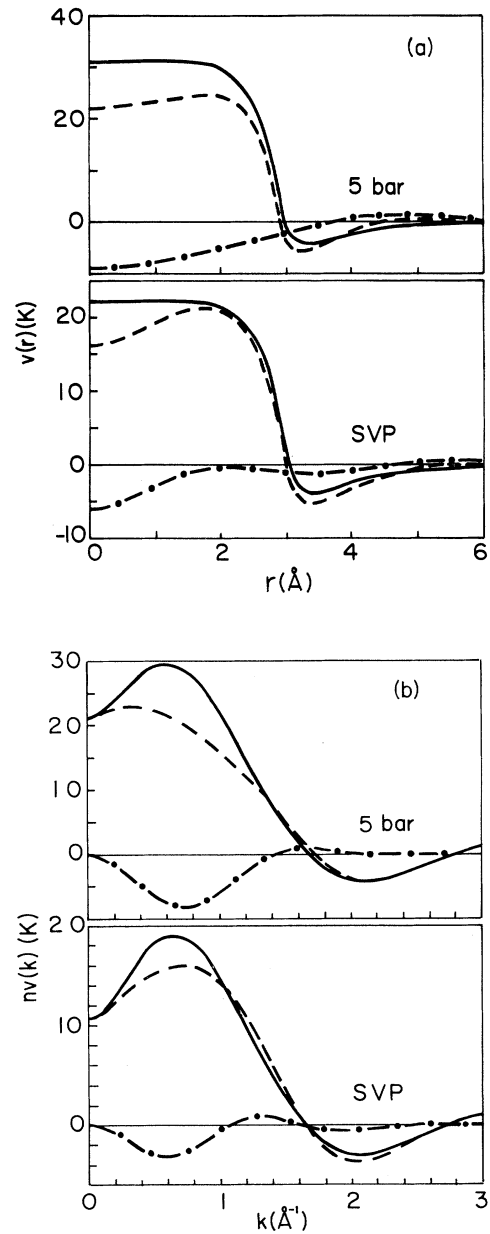


FIG. 4. Potentials: (a) $v(r)$ vs r ; (b) its Fourier transform $v(k)$ vs k at two pressures. Solid lines, HP potential; dashed-dotted lines, modification; dashed lines, modified potential (their sum).

Ref. 4.

The above considerations have demonstrated that the precise form of the potential is quite important in determining both the position and the width of the zero-sound mode. In fact, these considerations may help in determining a better potential than obtained hitherto. We might mention that after our calculations were completed, our attention was drawn to a remark by Levin and Valls³ in which they point out that Bedell and Pines,¹² in order to get a good agreement with the transport

coefficients and the superfluid transition temperature T_c in ^3He , were led to modify the Aldrich-Pines potential. It turns out that our modified potential [dashed curve of Fig. 4(b)] is quite close to the Bedell-Pines potential, as can be seen from Fig. 10 of Ref. 3. It seems to us that it will be possible to construct in the future a common potential which should be good for transport properties and T_c as well as for zero-sound dispersion and damping (Fig. 5).

IV. COMMENTS

Granting the ansatz [Eqs. (2.4) and (2.5)], the calculation of the imaginary part of the proper polarizability and hence of the zero-sound line shape is based on microscopic considerations. The merit of the ansatz is to be judged by the results it yields for the line shape, keeping in mind that this shape depends very sensitively on the potential. The latter is strongly dependent on pressure and wave number. In contrast to the other fermion systems, such as the electron gas, the situation in liquid ^3He is far from trivial since the linewidth of the zero-sound mode is comparable to its energy.

One might worry that, on one hand, we have added to Π_{HP} the imaginary contribution of the ten Feynman diagrams denoted by $i\text{Im}\Pi_{2p}$, and on the other hand, we have ignored adding the corresponding real part. It is so because we do not expect to improve the accuracy of the total $\text{Re}\Pi$ by adding $\text{Re}\Pi_{2p}$. In the first place, since this contribution arises from the second-order diagrams, it may introduce only a small correction to the dominant zero- and first-order diagrams. Secondly, we should keep in mind that besides the ten selected diagrams of Π_{2p} , there exist other second-order diagrams; and very often in the perturbation expansion some compensations occur among diagrams of the same order. It would, therefore, be unwise to include only a part of them. And finally, as it follows from HP formulation, their $\text{Re}\chi_{\text{sc}}$, incorporated by us [see Eqs. (2.8) and (2.7)], includes in a model form a multipair contribution, whose strength is fixed by HP by the requirement that χ_{sc} satisfy the f sum rule. Therefore, we may consider that our two-pair contribution $\text{Re}\Pi_{2p}$ is already approximately contained within their multipair term. The situation with the imaginary part for $\omega > \omega_{\text{SPE}}$ is, however, completely different: just the ten diagrams of $\text{Im}\Pi_{2p}$ provide the nonvanishing lowest-order contribution to $\text{Im}\Pi$, while the model multipair contribution of HP gives $\text{Im}\Pi_{\text{HP}}=0$ in this region of frequency.

A word about the ansatz equation (2.5) is in order. We have used m^* in the evaluation of the ten second-order diagrams, guided by the fact that, in the phenomenological approach of HP, m^* occurs in their χ_{sc} and hence in the Lindhard function—the empty bubble diagram. We did not incorporate the k dependence (which is weak in the considered k range) of the effective mass because there is no natural way of doing this within a perturbation approach.

A brief comment on our choice of f_k^s , the symmetric part of the Aldrich-Pines (or HP) scalar polarization potential for $v(k)$ [Eq. (2.4)], is in order. Short-range corre-

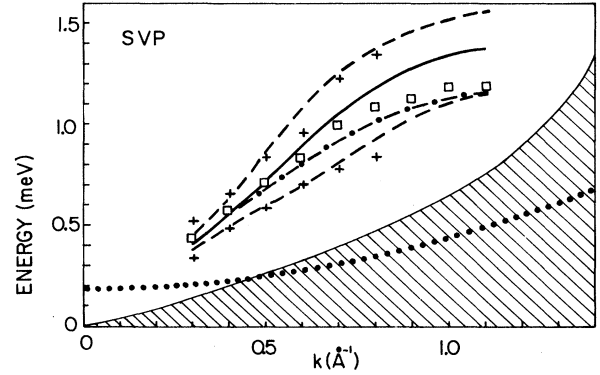


FIG. 5. Characteristic energies vs k at SVP calculated with modified potential. Solid line, position of the maximum; dashed lines, position at half maximum of the zero-sound peak; dashed-dotted line, zero-sound energy when damping is excluded. Experimental points from Ref. 4 are: squares, $\omega_0(k)$; crosses, $\omega_0(k) \pm \frac{1}{2}\Gamma(k)$; hatched area limited by $\omega_{\text{spe}}(k)$ single-pair excitation continuum; dotted line, $\omega_{\text{asym}}(k)$.

lations in liquid ^3He lead to a renormalization of the hard core of the bare potential resulting in a “weak” pseudopotential. It is very difficult, if not impossible, to calculate quantitatively from first principles this pseudopotential. The only choice left is to resort to a semi-phenomenological approach, and we have seen that the HP potential does the job admirably and hence our choice of f_k^s for $v(k)$. It is, indeed, a Lennard-Jones potential with a truncated hard core.

We have tacitly assumed that the contribution of processes involving more than two-particle-hole pairs to $\text{Im}\Pi$ is negligible. This contribution should be much smaller in the frequency range of interest since their asymptotic behavior involves higher inverse powers of frequency.

In the future, instead of using the asymptotic expression for the imaginary part of the proper polarizability, one should calculate it by evaluating numerically the multidimensional integrals. This could easily account for at least part of the discrepancy from experiment in the linewidth for both large and small wave numbers, and extend the validity of the calculation in the interesting region of wave numbers for which the dispersion is flat. Also, it would be very interesting to obtain an analytic expression for the linewidth in the limit $k \rightarrow 0$. It should be possible to extend the present calculation to the case of a fully polarized model liquid ^3He using the effective potential of Ng and Singwi.¹³

ACKNOWLEDGMENTS

This work was mostly carried out during our participation in the workshop on Condensed Matter Physics at the International Center for Theoretical Physics, Trieste, Italy. Our thanks are due to the Center for its hospitality and to Professor Mario Tosi for his interest in this work. We also wish to thank Dr. D. W. Hess for supplying us the numerical values of f_k^s for different pressures.

- ¹L. D. Landau, Zh. Eksp. Theor. Phys. **32**, 59 (1957) [Sov. Phys.—JETP **5**, 101 (1957)].
- ²K. Sköld, C. A. Pelizzari, R. Kelb, and G. O. Ostrowski, Phys. Rev. Lett. **37**, 842 (1976).
- ³See K. Levin and O. T. Valls, Phys. Rep. **98**, 1 (1983).
- ⁴R. Scherm, K. Guckelsberger, B. Fåk, K. Sköld, A. J. Dianoux, H. Godgrin, and W. G. Stirling, Phys. Rev. Lett. **59**, 217 (1987).
- ⁵C. H. Aldrich III and D. Pines, J. Low Temp Phys. **32**, 689 (1978).
- ⁶D. W. Hess and D. Pines, J. Low Temp. Phys. **72**, 247 (1988).
- ⁷A. Holas and K. S. Singwi, preceding paper, Phys. Rev. B **40**, 158 (1989).
- ⁸A. J. Glick and W. F. Long, Phys. Rev. B **4**, 3455 (1971).
- ⁹H. R. Glyde and F. C. Khanna, Can. J. Phys. **58**, 343 (1980).
- ¹⁰K. Gottfried and L. Pičkmán, K. Dan. Vidensk. Selsk. Mat. Fys. Medd. **32**, 13 (1960).
- ¹¹HP used for Landau parameters and density the experimental values of Greywall [Phys. Rev. B **27**, 2747 (1983)]. In their calculation for the highest pressure they used the values corresponding to a pressure of 18 bar. To avoid any confusion, we have marked correspondingly our results as pertaining to $p = 18$ bar, although HP use $p = 21$ bar for labeling their results.
- ¹²J. Bedell and D. Pines, Phys. Lett. **78A**, 281 (1980).
- ¹³Tai Nai Ng and K. S. Singwi, Phys. Rev. Lett. **57**, 226 (1986).